Available online at www.sciencedirect.com
SCIENCE DIRECT®
Inorganica Chimica Acta 345 (2003) 279–291
Inorganica Chimica Acta
www.elsevier.com/locate/ica

The role of bulky substituents in the polymerization of ethylene using late transition metal catalysts: a comparative study of nickel and iron catalyst systems

George J.P. Britovsek, Simon P.D. Baugh, Olivier Hoarau, Vernon C. Gibson *, Duncan F. Wass, Andrew J.P. White, David J. Williams

Department of Chemistry, Imperial College of Science, Technology and Medicine, South Kensington, London SW7 2AY, UK

Received 13 June 2002; accepted 28 June 2002

Dedicated in honor of Professor Richard R. Schrock

Abstract

A series of nickel(II) and iron(II) complexes of the general formula [LMX_2] containing bidentate (for M = Ni) and tridentate (for M = Fe) heterocycle-imine ligands L have been synthesized and characterized. Compared to the well-known α-diimine nickel and bis(imino)pyridine iron catalysts, these systems contain a bulky imine substituent on one side and a non-bulky N-heterocycle on the other. Depending on the ligand and the conditions used, either four- or five-coordinate complexes are obtained in the case of nickel. Iron complexes are generally five-coordinate, even with potentially tetradentate ligands. Activation of these precatalysts with MAO affords active catalyst systems for the oligomerization/polymerization of ethylene. Compared to α-diimine nickel and bis(imino)pyridine iron catalysts, both metal systems provide only half of the steric protection and consequently the catalytic activities and the degree of polymerization are significantly lower. Lower activities are attributed to a reduced stability of the active species under polymerization conditions, whereas the lower molecular weights are a result of increased β-H transfer rates. Variations within the heterocyclic component of the ligand reveal that both steric and electronic factors influence the polymerization behavior of these catalysts.

Keywords: Nickel; Iron; Polymerization; Ethylene; Polyethylene

1. Introduction

The field of olefin polymerization catalysis has made enormous advances during the last decade. In addition to the well established Ziegler–Natta and metallocene catalyst systems, several late transition metal based catalysts have shown great potential for the polymerization of ethylene [1–3]. Nickel α-diimine catalysts of type **A** (Fig. 1) [4–6] and bis(imino)pyridine iron catalysts of type **B** [7–12], when activated with MAO, are highly active for the polymerization of ethylene. In terms of understanding the underlying principles governing olefin polymerization, these late metal systems have re-emphasized the general characteristics believed to be responsible for highly active catalysts, such as electron deficiency and coordinative unsaturation at the metal center [1]. More significantly, these systems have also highlighted a relatively new factor that is now recognized to be of central importance for obtaining high activities and high molecular weight product in nickel and iron catalyst systems: *bulky aryl substituents*. For both types of catalysts, **A** and **B**, small aryl substituents result in the formation of low molecular weight oligomers [13–18], whereas bulky aryl substituents give high molecular weight polyethylene [5,11].

Unusual behavior of polymerization catalysts containing bulky substituents has been noted previously in a number of polymerization systems. Wu and Swift reported in 1972 that, in the oligomerization of isoprene with iron(II) catalysts containing iminopyridine ligands

* Corresponding author
E-mail address: v.gibson@ic.ac.uk (V.C. Gibson).

0020-1693/02/$ - see front matter
PII: S0020-1693(02)01293-8

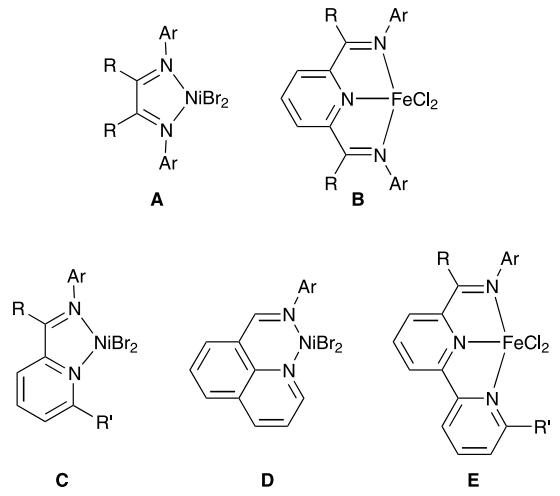

Fig. 1. Nickel and iron olefin polymerization precatalysts.

(ligands as in complex **C**, Fig. 1), the bulky 2,6-dimethylphenyl derivative showed an exceptionally high activity and selectivity for the cyclodimerization of isoprene, which was noted at the time as 'anomalous behavior' [19]. During the 1980s Keim reported nickel catalysts for the polymerization of ethylene that featured moderately bulky groups such as $SiMe_3$ and very bulky supermesityl substituents (see Fig. 2) [20,21]. However, variations on the substituents were not explored and the effect of bulky groups remained largely unremarked upon. It was not until the mid-1990s, when Brookhart and co-workers showed that nickel complexes with bulky α-diimine ligands afford highly active catalysts for the polymerization of ethylene, and that the degree of polymerization and activity is highly dependent on the substitution pattern of the aryl groups, that the bulky substituent effect became more obviously apparent. More recently, bulky aryl substituents have been used to give other highly active late transition metal ethylene polymerization catalysts, for example, systems containing [N,O], [P,O] and [P,P] ligands (see Fig. 2) [22–24].

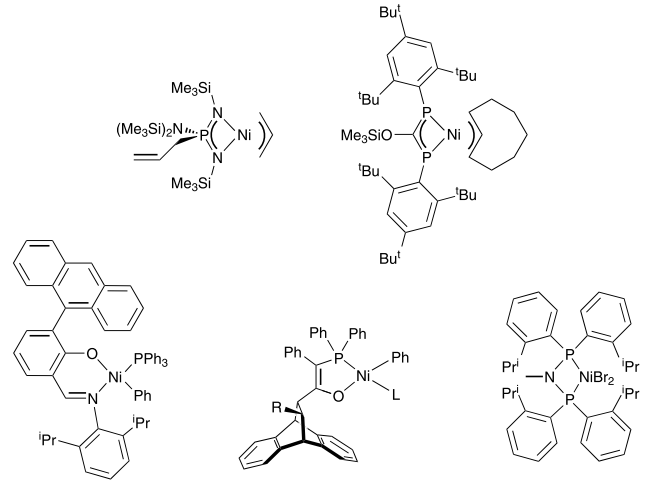

Fig. 2. Nickel catalysts with bulky substituents used in olefin polymerization.

As part of our ongoing research in the field of late transition metal olefin polymerization catalysis [11,18,25–28], we describe here the synthesis of a series of hybrid ligands containing a bulky arylimino substituent on one side of the ligand and a relatively unhindered heterocyclic donor on the other. These ligands thus provide only half of the steric protection of derivatives with bulky substituents on both donor atoms. The catalytic ethylene oligo- and polymerization properties of nickel and iron precatalysts, i.e. nickel complexes with bidentate imino-heterocycle ligands of types **C** and **D** and iron complexes with tridentate ligands of type **E** have been investigated and compared with the parent α-diimine nickel and bis(imino)pyridine iron precatalysts, with the aim of gaining a better understanding of the role and exceptional influence of bulky aryl substituents in polymerization catalysts.

2. Results and discussion

2.1. Synthesis of ligands

Bidentate imino-heterocycle ligands **1**–**4**, shown in Fig. 3, were synthesized by condensation of the parent anilines and heterocyclic aldehydes or ketones according to known procedures [29]. Pyrazine carboxaldehyde and 8-quinoline carboxaldehyde were prepared by selective oxidation of the corresponding methyl precursors [30,31].

The tridentate iminobipyridine ligand **5** was obtained by condensation of 6-acetyl-2,2′-bipyridine [32] with 2,6-

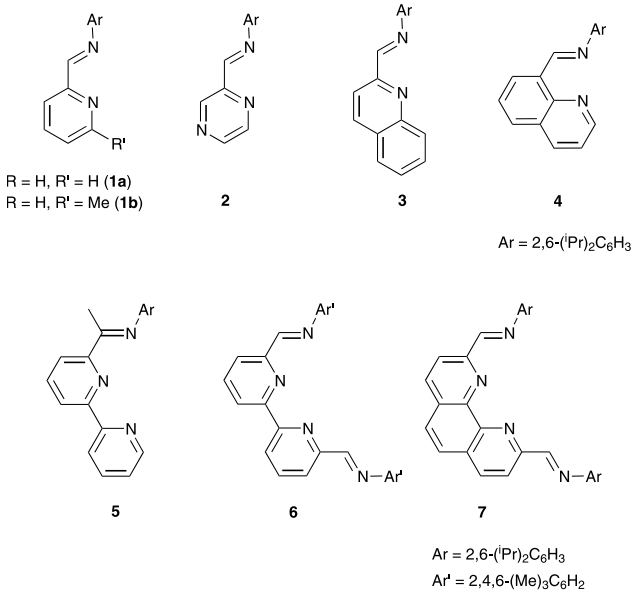

Fig. 3. Bidentate and tridentate nitrogen ligands used in this study.

diisopropylaniline [33]. The bis(imino)bipyridine and bis(imino)phenanthroline ligands **6** and **7** were prepared by selective oxidation of the methyl precursors to give 6,6′-diformyl-2,2′-bipyridine [34] and 2,9-diformyl phenanthroline [35], followed by condensation with the appropriate anilines (2,4,6-trimethylaniline in the case of **6** and 2,6-diisopropylaniline for **7**).

2.2. Synthesis of nickel complexes

Reaction of ligands **1**–**4** with (dme)$NiBr_2$ in dichloromethane produces orange nickel dibromide complexes in high yield. Elemental analysis is in all cases consistent with the stoichiometry (ligand)$NiBr_2$. ^1H NMR spectroscopy shows all complexes to be paramagnetic, giving broad contact-shifted peaks in the range −20 to 80 ppm, indicating that the complexes possess a tetrahedral geometry as seen for (α-diimine)$NiBr_2$ complexes [5]. Mass spectral data (FAB) show peaks due to both fragments $[(ligand)NiBr_2]^+$ and $[(ligand)NiBr_2]_2^+$, suggesting that dimeric complexes may have been formed. Indeed, five-coordinate dimeric structures for complexes $[(\mathbf{1a})NiBr_2]_2$ and $[(\mathbf{1b})NiBr_2]_2$ have been reported by Laine et al. [36,37]. We have confirmed the dimeric structure of $[(\mathbf{1a})NiBr_2]_2$ when crystallized from a saturated dichloromethane solution, but we have also found that the solid state structure of these iminopyridine nickel complexes is affected by the type of ligand and also by the solvent used for crystallization. Cooling a saturated acetonitrile solution of complex $[(\mathbf{1a})NiBr_2]$ yielded yellow/orange needles of a monomeric acetonitrile adduct. The molecular structure of $[(\mathbf{1a})NiBr_2(CH_3CN)]$ is shown in Fig. 4, with selected bond lengths and angles in Table 1. In this case, a preference for a five-coordinate complex is found with one acetonitrile molecule in the axial coordination site. Apparently, acetonitrile is a stronger donor than a bridging bromide. The binding of this solvent molecule also reflects the more open coordination environment afforded by the less bulky iminopyridine ligand compared to the α-diimine ligands.

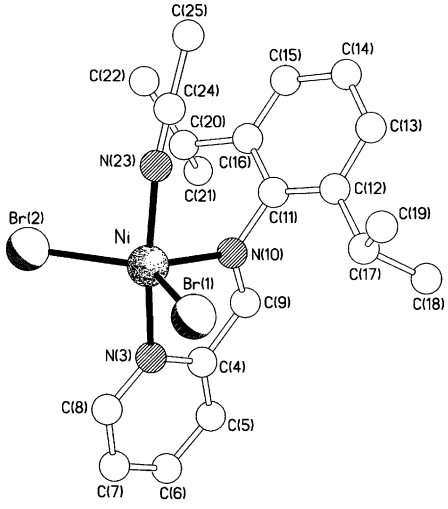

Fig. 4. The molecular structure of $[(\mathbf{1a})NiBr_2(MeCN)]$.

Table 1
Selected bond lengths (Å) and angles (°) for $[(\mathbf{1a})NiBr_2(MeCN)]$

Bond lengths			
Ni–N(23)	2.045(4)	Ni–N(3)	2.059(3)
Ni–N(10)	2.068(3)	Ni–Br(2)	2.4251(9)
Ni–Br(1)	2.4383(9)	C(9)–N(10)	1.261(5)
Bond angles			
N(23)–Ni–N(3)	169.6(2)	N(23)–Ni–N(10)	91.47(14)
N(3)–Ni–N(10)	78.78(12)	N(23)–Ni–Br(2)	91.23(12)
N(3)–Ni–Br(2)	92.29(9)	N(10)–Ni–Br(2)	129.67(9)
N(23)–Ni–Br(1)	92.19(13)	N(3)–Ni–Br(1)	93.78(9)
N(10)–Ni–Br(1)	105.11(9)	Br(2)–Ni–Br(1)	124.98(3)

The X-ray structure of $[(\mathbf{1a})NiBr_2(CH_3CN)]$ shows the geometry at nickel to be slightly distorted trigonal bipyramidal, the equatorial angles ranging between 105.11(9) and 129.67(9)°, the largest deviation from 120° being associated with N(10) and Br(1); the transaxial angle is 169.6(2)°. The equatorial coordination plane is planar to within 0.048 Å, and the nickel atom is displaced by 0.064 Å out of the N(10)/Br(1)/Br(2) plane in the direction of the coordinated acetonitrile ligand. The geometry of the chelating ligand is essentially unchanged from those observed in the closely related dimeric complexes $[(\mathbf{1a})NiBr_2]_2$ and $[(\mathbf{1a})NiCl_2]_2$ having a planar (to within 0.007 Å) chelate ring, a bite angle of 78.78(12)°, and with the 2,6-diisopropylphenyl ring system oriented approximately orthogonally (ca. 81°) to this plane [37]. This latter orientation facilitates a pair of C–H···N($p\pi$) interactions between the isopropyl methine hydrogen atoms [on C(17) and C(20)] and N(10), the H···N distances being 2.46 and 2.44 Å, respectively. The C(9)=N(10) bond length does not differ significantly from its counterparts in the related bromo- and chloro-dimers. The metal coordination distances are unexceptional and comparable to those in $[(\mathbf{1a})NiBr_2]_2$. The pyridyl rings of centrosymmetrically related molecules π-stack to form discrete 'dimers' with mean interplanar and ring centroid···centroid separations of 3.41 and 3.66 Å, respectively.

By contrast, the solid state structure of the quinolylimine nickel complex $[(\mathbf{3})NiBr_2]$ crystallized from dichloromethane, shows a monomeric four-coordinate complex with a tetrahedral geometry around the nickel center. No tendency to form a dimeric complex is seen, most likely a consequence of the larger in-plane steric demands of this ligand, as seen for α-diimine ligands [5]. The tetrahedral geometry at nickel (Fig. 5) is severely distorted in this case with angles ranging between 81.1(2) and 130.0(2)°, the acute angle being associated with the bite of the chelating ligand, and the obtuse with

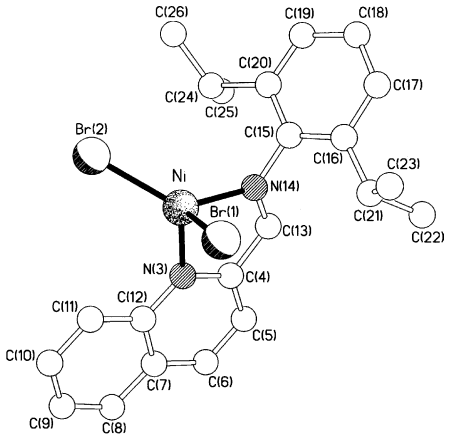

Fig. 5. The molecular structure of [(**3**)$NiBr_2$].

Br(2) and N(14). The replacement of the pyridine moiety by quinoline does not significantly effect the overall ligand conformation, the 2,6-diisopropylphenyl ring system still being oriented approximately orthogonally (ca. 77°) to the plane of the chelate ring; the associated isopropyl methine hydrogen···N(14) distances are here 2.37 and 2.47 Å. The deviation from planarity of the chelate ring is here 0.037 Å (cf. 0.007 Å in [(**1a**)$NiBr_2$(MeCN)]), though N(3)/C(4)/C(13)/N(14) are planar to within 0.005 Å, the nickel atom lying 0.132 Å out of this C_2N_2 plane (i.e. there is a slight folding of the ring). The C=N double bond length is unchanged (Table 2). The metal coordination distances to the two nitrogen atoms are both significantly shorter (by approximately 0.05 Å) than those seen in [(**1a**)$NiBr_2$(MeCN)] as are the two Ni–Br distances. A similar packing motif to that seen in [(**1a**)$NiBr_2$(MeCN)] is observed with π–π overlap of the quinoline rings of centrosymmetrically related pairs of molecules; the mean interplanar and ring centroid···centroid separations are 3.45 and 3.62 Å, respectively.

Two well-defined cationic nickel alkyl complexes $[(\mathbf{1a})NiMe]^+$ and $[(\mathbf{2})NiMe]^+$ have been synthesized in two steps from the parent dibromide complexes according to Scheme 1. Treatment of [(**1a**)$NiBr_2$] and [(**2**)$NiBr_2$] with methylmagnesium bromide gives the highly air and moisture sensitive dimethyl complexes [(**1a**)$NiMe_2$] and [(**2**)$NiMe_2$] in good yield. The diamagnetic nature of these complexes indicates a square planar geometry, in contrast to their dibromide precursors. Treatment of the dimethyl complexes with $[H(OEt_2)_2]BArF$ ($BArF = [B(3,5\text{-}(CF_3)_2C_6H_3)_4]^-$) results in the evolution of methane by protonation of one methyl ligand and formation of the cationic complexes as diethylether adducts in near quantitative yield by ^1H NMR spectroscopy. These complexes are extremely air and moisture sensitive and decompose slowly (half-life approximately 30 min) in d_2-dichloromethane solution at room temperature, even under an inert atmosphere. Again, the diamagnetism of these complexes suggests a square planar geometry. Only one of the two possible isomers, i.e. with heterocycle or imine donor *trans* to the methyl group, was observed. The structure is presumed to be the isomer with *trans* heterocycle and methyl groups, as observed in palladium analogues [38].

Table 2
Selected bond lengths (Å) and angles (°) for [(**3**)$NiBr_2$]

Bond lengths			
Ni–N(14)	2.010(5)	Ni–N(3)	2.014(5)
Ni–Br(2)	2.3049(13)	Ni–Br(1)	2.3538(13)
C(13)–N(14)	1.266(8)		
Bond angles			
N(14)–Ni–N(3)	81.1(2)	N(14)–Ni–Br(2)	130.0(2)
N(3)–Ni–Br(2)	117.3(2)	N(14)–Ni–Br(1)	101.3(2)
N(3)–Ni–Br(1)	108.2(2)	Br(2)–Ni–Br(1)	113.74(5)

2.3. Synthesis and characterization of iron complexes

Reaction of the ligands **5**–**7** with iron dichloride in n-butanol or thf affords the corresponding iron complexes in high yield. The compounds are sparingly soluble in common organic solvents, preventing NMR analysis, but have been characterized by mass spectrometry, microanalysis and magnetic moment. These data support the formulation of the complex as $LFeCl_2$. The bulky aryl substituent prevents the formation of bis-chelate complexes of the type $[L_2Fe][FeCl_4]$, which have been reported for smaller substituents [39,40]. Magnetic moments are typical for high spin iron(II) complexes with four unpaired electrons. Based on these experimental data, complex [(**5**)$FeCl_2$] is most likely a five-coordinate complex, similar to the many structures we have determined for bis(imino)pyridine iron and cobalt complexes [11,18,26]. The bis(imino)bipyridine and bis(imino)phenanthroline ligands **6** and **7** can coordinate as tridentate, tetradentate or bridging bidentate ligands [41–43]. The IR spectrum of complex [(**7**)$FeCl_2$] shows two bands, one for the uncoordinated C=N stretch (1635 cm^{-1}, cf. 1639 cm^{-1} in the free ligand) and another for the coordinated C=N stretch at 1615 cm^{-1}, indicating that the ligand acts as a tridentate ligand. The IR spectrum of complex [(**6**)$FeCl_2$] is less clear. A broad absorption is observed at 1634 cm^{-1}, partly overlapping with a strong band at 1592 cm^{-1}, which probably obscures the absorption attributable to the coordinated imine. Mass spectrometry and magnetic moment measurements suggest the formulation $LFeCl_2$. Crystallographic analysis of complex [(**6**)$FeCl_2$] indeed supports this formulation whereby only one imine donor coordinates to the metal center (see Fig. 6).

The geometry at iron in complex [(**6**)$FeCl_2$] can probably be best described as severely distorted trigonal bipyramidal with N(2) and N(3) occupying the axial

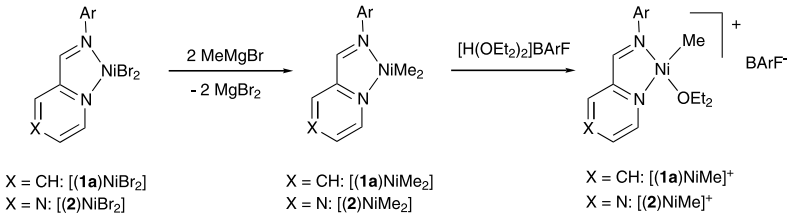

Scheme 1.

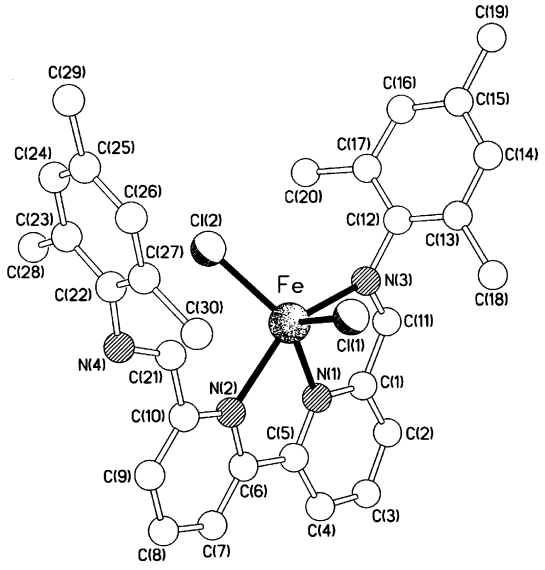

Fig. 6. The molecular structure of [(**6**)$FeCl_2$].

sites and N(1), Cl(1) and Cl(2) forming the equatorial plane. The equatorial angles range between 113.35(10) and 131.9(2)°, and the transaxial angle is 148.5(3)°, the deviation from linearity being a consequence of the two chelate bite angles (Table 3). In common with the structures of [(**1a**)$NiBr_2$(MeCN)] and [(**3**)$NiBr_2$] discussed above, [(**6**)$FeCl_2$]) has approximate C_s molecular symmetry, having a near planar ligand backbone with the terminal mesityl ring systems oriented nearly orthogonally (approximately 78 and 80°). The C=N distances for the coordinated and non-coordinated imino moieties are 1.275(11) and 1.236(12) Å, respectively, the shorter length reflecting the absence of coordination of the imino nitrogen atom. There is a small out of plane twist (approximately 6°) within the bipyridyl portion of the ligand. The N(1)/N(3) containing chelate ring is planar to within 0.019 Å whereas the N(1)/N(2) containing ring deviates by 0.038 Å. The metal coordination distances are overall very similar to those reported for 2,6-bis[1-(2,6-diisopropylphenylimino)ethyl]iron(II) chloride [11], the only significant difference being a lengthening by approximately 0.03 Å of the two 'axial' Fe–N distances, although the coordination geometry is noticeably different (distorted trigonal bipyramidal in [(**6**)$FeCl_2$] versus distorted square based pyramidal) [11]. The packing of the molecules in this structure contains a more extensive pattern of π–π stacking interactions than was seen in either [(**1a**)$NiBr_2$(MeCN)] or [(**3**)$NiBr_2$]. The bipyridyl rings of centrosymmetrically related pairs of molecules mutually overlap (mean interplanar and ring centroid···centroid separations of approximately 3.53 and 3.68 Å, respectively), this stacking motif extending to include the mesityl ring of the non-coordinated ligand arm of the ligand which overlays the N(1) containing pyridyl ring of a symmetry related complex (mean interplanar and ring centroid···centroid separations of approximately 3.48 and 3.78 Å, respectively) to create a continuous chain of π–π linked complexes.

Table 3
Selected bond lengths (Å) and angles (°) for [(**6**)$FeCl_2$]

Bond lengths			
Fe–N(1)	2.108(7)	Fe–N(3)	2.266(8)
Fe–Cl(2)	2.272(3)	Fe–N(2)	2.282(8)
Fe–Cl(1)	2.323(3)	N(3)–C(11)	1.275(11)
N(4)–C(21)	1.236(12)		
Bond angles			
N(1)–Fe–N(3)	74.8(3)	N(1)–Fe–Cl(2)	131.9(2)
N(3)–Fe–Cl(2)	102.8(2)	N(1)–Fe–N(2)	73.8(3)
N(3)–Fe–N(2)	148.5(3)	Cl(2)–Fe–N(2)	99.6(2)
N(1)–Fe–Cl(1)	114.7(2)	N(3)–Fe–Cl(1)	96.6(2)
Cl(2)–Fe–Cl(1)	113.35(10)	N(2)–Fe–Cl(1)	94.4(2)

3. Polymerization results

3.1. Ethylene polymerization using nickel complexes (*L*)$NiBr_2$

The ethylene polymerization activity of the nickel and iron dihalide complexes was investigated using MAO as co-catalyst. The activity values and polymer data are reported in Table 4, together with data for the two single-component $[LNiMe]^+$ catalysts. Alkylaluminium halides ($Et_3Al_2Cl_3$ or Et_2AlCl) also yield active catalytic systems and indicate the tolerance of these iminopyridine catalysts to a wide variety of activating agents, similar to α-diimine systems [44].

Table 4
Results of ethylene polymerization with nickel and iron precatalysts

Run	Precatalyst (μmol)	MAO (mmol/equivalents)	Yield (g)	Activity (g mmol^{-1} h^{-1} bar^{-1})	M_w [d]	M_n [d]	M_w/M_n	α
1 [a]	[(**1a**)NiBr$_2$] (10)	2/200	3.46	690	540	310	1.7	
2 [a]	[(**1b**)NiBr$_2$] (10)	2/200	0.20	40	300	140	2.1	
3 [a]	[(**2**)NiBr$_2$] (10)	2/200	trace	< 1				
4 [a]	[(**3**)NiBr$_2$] (10)	2/200	1.3	260	oligomers			
5 [a]	[(**4**)NiBr$_2$] (10)	2/200	0.06	6				
6 [b]	[(**1a**)NiMe]$^+$ (10)		1.1	110	350	210	1.7	
7 [b]	[(**2**)NiMe]$^+$ (10)		0.6	60	2100	1000	2.1	
8 [c]	[(**5**)FeCl$_2$] (6)	1.2/200	17.1 [e]	570	oligomers			0.35 [e]

[a] Toluene solvent, 1 bar, 30 min, 25 °C.
[b] Dichloromethane solvent, 1 bar, 60 min, 0 °C.
[c] Isobutane solvent, 5 bar, 1 h, 50 °C, scavenger MAO.
[d] Determined by GPC at 135 °C.
[e] Determined by GC.

The activity of the iminopyridine catalyst [(**1a**)NiBr$_2$] was found to be 690 g mmol^{-1} h^{-1} bar^{-1}, which is considerably lower than the activities seen for (α-diimine)NiBr$_2$ catalysts of type **A** where R = H and Ar = 2,6-diisopropylphenyl (Fig. 1) [4]. The molecular weight of the polyethylene product is also significantly lower (M_w = 540 vs. 76 000) [4]. Compared to the iminopyridine catalyst [(**1a**)NiBr$_2$], the 6-methyl derivative [(**1b**)NiBr$_2$] shows much reduced activity (40 g mmol^{-1} h^{-1} bar^{-1}, run 2) and a lower molecular weight than for [(**1a**)NiBr$_2$], in accord with the observations of Laine et al. [37]. The in-plane steric bulk of the 6-methyl group seems to play an important role in determining the activity of this catalyst. To explore this effect further, we also synthesized and tested complex [(**3**)NiBr$_2$], which contains a quinolyl instead of a pyridyl moiety (run 4). This complex was previously reported as inactive for the polymerization of ethylene [45]. However, under the conditions used here, we found that this catalyst converts ethylene with good activity, but mainly to butenes and hexenes, i.e. an even more dramatic decrease in product molecular weight. Noteworthy, a much lower activity has been observed for the 2,2′-biquinoline derivative [46].

The 8-quinoline derivative [(**4**)NiBr$_2$] was synthesized to probe the effect of a larger chelate bite angle on the polymerization activity. In this case, a six-membered chelate ring is formed compared to the five-membered rings in the other nickel complexes. A very low activity of 6 g mmol^{-1} h^{-1} bar^{-1} was obtained with this catalyst under standard conditions (run 5). Low activities have also been reported for related β-diimine nickel catalysts of type **F** (Fig. 7) [47]. Whereas the difference in catalytic activity between β- and α-diimine nickel catalysts may be related to the lack of planarity and delocalization in the six-membered ring (the ligand adopts a boat conformation in **F**), this explanation can be ruled out for type **H** as the 2-quinolyl imine ligand **4** is likely to be planar, as seen in the crystal structure of

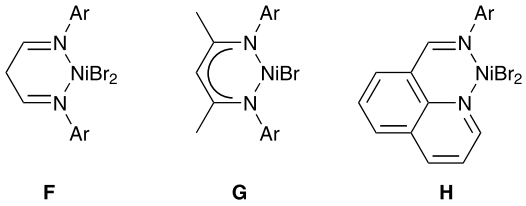

Fig. 7. Nickel complexes containing six-membered chelate rings.

precatalyst [(**3**)NiBr$_2$] (vide infra). In addition, very low activities have also been observed in the case of the planar β-diketiminate nickel catalysts **G**, which also feature a six-membered ring and bulky groups on each nitrogen donor [48]. However, these systems form neutral catalysts which are often less active than cationic systems. The difference in activity is therefore most likely to be the result of chelate ring size, whereby five-membered chelates generate more active catalysts than six-membered chelates.

The pyrazine derivative [(**2**)NiBr$_2$] is sterically identical to the active precatalyst [(**1a**)NiBr$_2$]. It therefore seems surprising that this complex shows no polymerization activity upon activation with MAO (run 3). It is possible that the reduced basicity of the pyrazine nitrogen donor (pK_a = 0.4 vs. 5.2 for pyridine) [58] may lead to catalyst deactivation (via ligand dissociation). Another possibility is coordination of the remote nitrogen donor of the pyrazine moiety to Lewis-acidic aluminium centers of the co-catalyst, which could also lead to catalyst deactivation. We therefore synthesized well-defined nickel alkyl complexes that do not require the presence of a Lewis acidic co-catalyst. Both single-component catalysts [(**1a**)NiMe]$^+$ and [(**2**)NiMe]$^+$ prove to be active ethylene polymerization catalysts (runs 6 and 7), though [(**1a**)NiMe]$^+$ is less active than its MAO-activated counterpart, possibly due to the absence of excess MAO to act as a poison scavenger for the more sensitive cationic alkyl system. The observation of activity for [(**2**)NiMe]$^+$ provides strong support for

the co-catalyst interfering with the ligand, leading to catalyst deactivation.

3.2. Analysis of polyethylene produced with nickel catalysts

In contrast to the high molecular weight polymer formed by α-diimine nickel catalysts of type **A** (R = H, Ar = 2,6-diisopropylphenyl) [4], the polymer materials generated by iminopyridine nickel catalysts are essentially low molecular weight, highly branched polyethylenes. These highly branched materials resemble the polyolefins formed by the polymerization of feedstocks such as isobutylene [49,50], more than traditional grades of polyethylene. Poly(isobutylene) has many applications and are among the most important compounds currently employed as engine lubricant additives. The molecular weights are only slightly higher than materials normally considered to be oligomers and are typically characterized using GC–MS and Schulz–Flory analysis. However, the materials described here contain a large number of isomers for each C_n-fraction because of chain branching and olefin isomerization. This hinders standard oligomer analysis by GC and requires polymer characterization techniques (GPC and NMR), which deal with averaged characteristics. Low molecular weights are believed to be obtained because imino-heterocycle ligands provide only half of the *ortho* aryl steric protection compared to symmetric α-diimine ligands. This reduced steric protection of the square planar catalysts' axial coordination sites is expected to lead to higher rates of chain transfer compared to α-diimine systems.

Runs 1 and 2 explore the differences in polymerization behavior between pyridyl and 6-methyl pyridyl derivatives with identical imine substitution patterns [(**1a**)$NiBr_2$] and [(**1b**)$NiBr_2$]. The polymer from run 1 has a molecular weight $M_w = 540$, which represents a material with an average chain length of approximately C_{35}. The polyethylene obtained from run 2 is slightly lower molecular weight; a value of $M_w = 300$ represents a C_{20} material. The polydispersities (M_w/M_n) for both materials are narrow and branching levels are similar. A more detailed breakdown of the types of branching present is problematic because polymer chain ends are indistinguishable from branches, which leads to a large overestimation in the amount of long (C_6+) branches for such low molecular weight materials. Examination of the DEPT 90 spectra of the polymers reveals that by far the largest CH signal is that assigned to methyl branches which suggests that the predominant branching features are methyl groups.

The most dramatic difference between the materials is found upon examination of the distribution of olefinic groups (see Table 5). Although both polymers contain predominantly internal olefins, the material from run 2 shows a much higher percentage of vinyl end groups (25.3%) compared to run 1 (6.5%). An increase in terminal unsaturation has important consequences for applications of poly(isobutylene) materials, which often require polymer chain-end functionalization. The 6-methyl group of compound [(**1b**)$NiBr_2$] clearly has a profound effect on the polymer produced, presumably by influencing the β-elimination/reinsertion mechanisms (chain walking) which lead to chain isomerization and the thermodynamically favored internal olefins. One possibility is that the in-plane steric bulk of this substituent disfavors the rotation of intermediate olefin complexes, which is necessary for the chain walking mechanism to operate. Since coordinated ethylene must also rotate into a co-planar orientation to undergo insertion this would also account for the low activity observed for this catalyst.

The material synthesized using the well-defined cation [(**1a**)NiMe]$^+$ (run 6) closely resembles the polyethylene obtained by MAO activation of the related dibromide catalyst [(**1a**)$NiBr_2$] (run 1), albeit with slightly lower molecular weight. This is attributable to the differences in temperature at which these experiments were performed and/or the nature of the activation method/anion used. Anion influences on polymer structure have been reported for palladium diimine catalysts [47]. Comparison of the materials obtained from runs 6 and 7 (Table 4) shows a significant increase in molecular weight using the pyrazyl-imine catalyst [(**2**)NiMe]$^+$ compared to the iminopyridine catalyst [(**1a**)NiMe]$^+$. The material from run 7 also proves to be more linear. As well as both polymerization runs being performed under identical conditions, the well-defined cationic catalysts have identical steric constraints. The only difference between the two catalysts is the electronic difference between the pyridyl and pyrazyl groups. Thus, runs 6 and 7 show an example of *electronic influence* over polymer structure. Electronic control in polymerization/oligomerization has been reported for neutral nickel catalysts supported by anionic pyridine carboxylate and pyrazine carboxylate ligands. In this case a change of mechanism is proposed to be responsible [51]. Comparison of the pK_a of pyridine and pyrazine (5.2 and 0.4, respectively) [58] reveals the additional nitrogen of the pyrazine heterocycle has an electron withdrawing effect. It is possible that this electron withdrawing effect influences (reduces) the overall rate of β-H elimination, which would lead to the observed higher molecular weight, and more linear, material. Another possibility, which has been proposed by Ziegler and co-workers for diimine systems, involves electron withdrawing substituents enhancing a torsional role of the bulky aryl groups, which aids chain propagation and disfavors branching and chain transfer [52]. By whatever mechanism it is asserted, electronic control in late transition metal systems could offer a

Table 5
Polymer analysis results for runs 1,2 and 6

Run	Precatalyst	Branches [a]			Olefinic groups [a]		
		Me	Et	>Bu	Vinyl	2-Alkene	>3-Alkene
1	[(**1a**)$NiBr_2$]	7.3	1.8	8.7	6.5	35.2	50.0
2	[(**1b**)$NiBr_2$]	9.7	3.4	11.0	25.3	32.7	34.3
6	[(**1a**)NiMe]$^+$	8.9	2.9	10.9	3.6	37.8	47.3

[a] Determined by ^{13}C NMR. Values given are as % of total number of carbons.

useful additional handle to supplement the more usual steric methods for influencing polymer microstructure.

3.3. Ethylene polymerization using iron complexes (L)$FeCl_2$

The catalytic potential of the iron complexes containing tridentate ligands has been evaluated using MAO as the co-catalyst [33,53]. From Table 4 (run 8) it can be seen that, compared to the parent bis(imino)pyridine iron catalyst which is highly active and produces high molecular weight polyethylene (Act. > 5000 g mmol^{-1} h^{-1} bar^{-1}, M_w > 500 000) [11], the imino bipyridine derivative [(**5**)$FeCl_2$] shows a lower activity of 570 g mmol^{-1} h^{-1} bar^{-1} and produces very low molecular weight oligomers. This complex shows similar behavior to the previously reported oligomerization catalysts, containing bis(imino)pyridine ligands with small aryl substituents [18]. The product mixture consists of mainly 1-butene and 1-hexene and follows a typical Schulz–Flory type distribution with a very low α-value of 0.35. Apparently, a big aryl substituent on one side of the complex and the absence of steric protection on the other side has an even more dramatic effect than having a small aryl substituent on each side.

In the case of the complexes [(**6**)$FeCl_2$] and [(**7**)$FeCl_2$], which contain a tridentate imino bipyridine and an imino phenanthroline ligand with a pendant imino substituent, respectively, no catalytic activity was observed upon activation with MAO. It could be argued that the pendant imino donor can coordinate to the metal center in the activated species, thereby blocking a coordination site on the metal that may be needed for catalysis [42]. However, we have shown recently that bis(imino)pyridine iron and cobalt complexes containing additional donors such as acetonitrile or thf do not significantly affect the catalytic performance of these catalysts [27]. We believe that, similar to the case of the nickel complex [(**1b**)$NiBr_2$] described earlier, this lack of activity may be related to the in-plane steric bulk created by the *ortho* substituent on the second pyridyl unit.

4. Mechanistic considerations

In the case of nickel α-diimine catalysts, Brookhart and co-workers have shown that the catalyst resting state is a nickel alkyl olefin complex [5]. The rate determining step in the catalytic cycle is the migratory insertion of ethylene into the metal alkyl bond, and therefore the rate of propagation for these catalyst systems shows a zero order dependence on ethylene. Ziegler has suggested that chain transfer via transfer to monomer is suppressed by bulky substituents, which destabilize the transition state and thereby increase the activation barrier for this chain transfer process [52,54]. Thus, smaller substituents should lead to lower molecular weight products, which is supported by our results on the unsymmetrical ligand–nickel systems reported here.

These same arguments may apply to bis(imino)pyridine iron catalysts, although the resting state of the catalyst is likely to be different. We have shown previously that the rate of propagation for these catalysts shows a first order dependence on ethylene [11], which indicates that the rate determining step must involve ethylene. We therefore propose that the catalyst resting state is an iron alkyl species and that the rate determining step is ethylene coordination to the iron center. This would imply that catalysts containing less sterically demanding ligands should provide easier access to the metal center and thus should give higher activities. However, reducing the steric protection of the metal center can lead to more rapid decomposition of the active species. Indeed, the activity profile of run 8 (ethylene flow vs. time) shows a much faster deactivation of the catalyst compared to typical bis(imino)pyridine iron catalysts and we believe this to be responsible for the lower activities found for [(**5**)$FeCl_2$]. The rate of chain transfer via transfer to monomer is first order in ethylene and more bulky substituents will decrease this rate, leading to higher molecular weight polyethylene [11]. Reducing the sterics, either on both sides or only on one side as described here, results in effectively only half of the steric protection and therefore in lower activities and lower molecular weight products.

5. Experimental

5.1. General

All manipulations were carried out under an atmosphere of nitrogen using standard Schlenk and cannula techniques or in a conventional nitrogen filled glove box. Solvents were refluxed over an appropriate drying agent, and distilled and degassed prior to use. Elemental analyses were performed by the microanalytical services of the Department of Chemistry at Imperial College and Medac Ltd. NMR spectra were recorded on a Bruker spectrometer: ^{1}H (250 MHz) and ^{13}C (62.9 MHz) at 293 K; chemical shifts are referenced to the residual protio impurity of the deuterated solvent. Polyethylene NMR spectra were recorded on a JEOL GSX270 for the following nuclei shown (frequencies in parentheses): ^{1}H (270.05 MHz) and ^{13}C (67.51 MHz). Mass spectra were obtained using VG Autospec or VG Platform II Mass Spectrometers for fast atom bombardment (FAB), electron impact (EI) or chemical ionization (CI). Gel permeation chromatographs (GPC) were obtained using a Waters 150CV (columns supplied by Shodex (807, 806 and 804)) (BP Chemicals Ltd.) at 135 °C. IR spectra were recorded on a Perkin–Elmer Spectrum GX1 System FTIR spectrometer. Magnetic susceptibility measurements have been performed using an Evans' balance.

The synthesis of some pyridyl imine ligands (**1a**–**b**, and **3**) together with the corresponding Ni complexes has been reported previously [28,36,38,55,56]. $[H(OEt_2)_2]BArF$ ($BArF = [B(3,5\text{-}(CF_3)_2C_6H_3)_4]^-$) [57], pyrazine carboxaldehyde [30], 8-quinoline carboxaldehyde [31], 6-acetyl-2,2′-bipyridine and the precursors 2-acetyl-6-bromopyridine and 2-(2′-methyl-1′,3′-dioxolane-2′-yl)-6-bromopyridine [32] were prepared according to literature procedures. The full procedure for the synthesis of ligand **5** has been disclosed previously [33]. The precursors for ligands **6** and **7**, 6,6′-diformyl-2,2′-bipyridine [34] and 2,9-diformyl phenanthroline [35], were synthesized by selective oxidation of the methyl precursors. MAO (10% solution in $C_6H_5CH_3$) was obtained from Aldrich. All other chemicals were obtained commercially and used as received unless stated otherwise.

5.2. Synthesis of ligands

5.2.1. [(2,6-Diisopropylphenylimino)methyl]pyrazine (2)

A discrete mixture of 2,6-diisopropylaniline (1.6 g, 9 mmol) and 2-pyrazinecarboxaldehyde (1.0 g, 9 mmol) was stirred for 1 h. During this time the mixture became viscous and heat was evolved. Pentane (approximately 50 ml) was added and the resultant yellow solution dried over anhydrous Mg_2SO_4. The solution was then filtered, concentrated and cooled to −30 °C. Compound **2** was isolated as large yellow blocks in 83% yield (2.0 g).

^{1}H NMR (250 MHz, $CDCl_3$, 298 K): δ 9.52 (s, 1H, 3-pyz–*H*), 8.72–8.62 (m, 2H, pyz–*H*), 8.38 (s, 1H, N=C*H*), 7.22–7.12 (m, 3H, Ar–*H*), 3.00 (sept, 2H, $J = 6.7$ Hz, C*H*(CH_3)$_2$), 1.20 (d, 12H, $J = 6.7$ Hz, CH(C*H*$_3$)$_2$). ^{13}C NMR (63 MHz, $CDCl_3$, 298 K): δ 161.5 (imine–*C*), 149.2, 148.1, 145.9, 144.2, 143.6, 137.1, 124.9, 123.2 (pyz– and Ar–*C*), 28.1 (*C*HMe$_2$), 23.5 (CH(*C*H$_3$)$_2$). IR (Nujol, NaCl, cm^{-1}): 1641(s), 1578(m), 1541(w), 1406(m), 1379(vs), 1365(s), 1349(m), 1321(w), 1300(w), 1266(w), 1255(w), 1179(s), 1162(m), 1108(w), 1052(m), 1016(s), 982(w), 967(w), 933(w), 876(m), 856(w), 847(w), 835(w), 807(w), 796(m), 755(m), 723(m), 708(w). MS (EI, *m*/*z*): 267 $[M]^+$. Elemental analysis for $C_{17}H_{21}N_3 \cdot 0.5H_2O$ (276.38) found (required): C, 73.59 (73.87); H, 7.94 (8.02); N, 15.00% (15.20).

5.2.2. 2-[(2,6-Diisopropylphenylimino)methyl]quinoline (3)

To a solution of 2,6-diisopropylaniline (0.81 g, 4.58 mmol) and 2-quinolinecarboxaldehyde (0.72 g, 4.58 mmol) in 10 ml CH_2Cl_2 was added a drop of formic acid and $MgSO_4$. The mixture was stirred at room temperature (r.t.) overnight. After filtration, the solvent was removed and the product recrystallized from warm C_6H_{14}. Compound **3** was isolated as a yellow solid in 77% yield (1.11 g).

^{1}H NMR (250 MHz, $CDCl_3$, 298 K): δ 8.51 (s, 1H, N=C*H*), 8.46–7.60 (m, 6H, quin–*H*), 7.25–7.17 (m, 3H, Ar–*H*), 3.04 (sept, 2H, $J = 6.7$ Hz, C*H*(CH_3)$_2$), 1.22 (d, 12H, $J = 6.7$ Hz, CH(C*H*$_3$)$_2$). ^{13}C NMR (63 MHz, $CDCl_3$, 298 K): δ 163.4 (imine–*C*), 154.6, 148.5, 148.0, 137.1, 136.7, 129.9, 129.1, 127.8, 124.5, 123.1, 118.3 (quin– and Ar–*C*), 28.0 (*C*HMe$_2$), 23.4 (CH(*C*H$_3$)$_2$). Elemental analysis for $C_{22}H_{24}N_2$ (316.45) found (required): C, 83.67 (83.50); H, 7.64 (7.64); N, 8.67% (8.85).

5.2.3. 8-[(2,6-Diisopropylphenylimino)methyl]quinoline (4)

An analogous procedure to that described for **3** was followed using 2,6-diisopropylaniline (0.56 g, 3.2 mmol) and 8-quinolinecarboxaldehyde (0.5 g, 3.2 mmol). Compound **4** was isolated as a yellow solid in 80% yield (0.8 g).

^{1}H NMR (250 MHz, $CDCl_3$, 298 K): δ 9.73 (s, 1H, N=C*H*), 8.98, 8.75, 8.20, 8.01, 7.75, 7.47 (m, 1H each, quin–*H*), 7.27–7.12 (m, 3H, Ar–*H*), 3.15 (sept, 2H, $J = 6.7$ Hz, C*H*(CH_3)$_2$), 1.28 (d, 12H, $J = 6.7$ Hz, CH(C*H*$_3$)$_2$). ^{13}C NMR (63 MHz, $CDCl_3$, 298 K): δ 160.6 (imine–*C*), 150.3, 150.1, 147.1, 137.7, 136.0, 133.0, 130.9, 128.2, 127.3, 126.5, 124.0, 122.9, 121.3 (quin– and Ar–*C*), 28.0 (*C*HMe$_2$), 23.5 (CH(*C*H$_3$)$_2$). IR (Nujol, NaCl, cm^{-1}): 1733(w), 1678(w), 1626(s), 1608(m), 1592(w), 1573(m), 1499(m), 1463(s), 1379(s), 1361(m), 1317(m), 1265(w), 1254(m), 1243(m), 1209(w), 1186(w),

1162(w), 1112(w), 1081(w), 1060(w), 1047(w), 1034(w), 936(w), 891(m), 832(m), 795(s), 770(w), 760(m), 745(m). MS (EI, *m/z*): 317 $[M]^+$. Elemental analysis for $C_{22}H_{24}N_2 \cdot 0.25H_2O$ (320.95) found (required): C, 82.42 (82.33); H, 7.71 (7.69); N, 8.74% (8.73).

5.2.4. 6-[1-(2,6-Diisopropylphenylimino)ethyl]-2,2′-bipyridine (**5**)

To a solution of 6-acetyl-2,2′-bipyridine (0.45 g, 2.27 mmol) in warm EtOH (1.5 ml) was added glacial AcOH (five drops), 4 Å mol sieves and 2,6-diisopropylaniline (0.53 g, 3.00 mmol). This mixture was heated to reflux for 15 h, during which time a solid precipitated. The mixture was cooled, filtered and the solid washed with EtOH (3 ml) to give the product as a light yellow solid in 87% yield (0.71 g).

^{1}H NMR ($CDCl_3$): δ 8.72 (dd, $J = 0.9$, 4.0 Hz, 1H, pyr*H*), 8.60–8.55 (m, 2H, pyr*H*), 8.43 (d, $J = 7.8$ Hz, 1H, pyr*H*), 7.96 (t, $J = 7.8$ Hz, 1H, pyr*H*), 7.84 (t, $J = 7.8$ Hz, 1H, pyr*H*), 7.36–7.31 (m, 1H), 7.22–7.13 (m, 3H, Ar*H*), 2.81 (sept, $J = 6.8$ Hz, 2H, C*H*$(CH_3)_2$), 2.36 (s, 3H, H_3CC=N), 1.19 (d, $J = 6.8$ Hz, 12H, CH(CH_3)$_2$). ^{13}C NMR ($CDCl_3$): δ 167.1 (*C*=N), 156.1, 155.7, 154.9, 149.2, 146.6, 137.4, 136.9, 135.8, 123.8, 123.6, 123.0, 122.0, 121.2, 121.1 (Ar*C* and pyr*C*), 28.3 (*C*H$(CH_3)_2$), 23.2, 22.9 (CH(*C*H_3)$_2$), 17.2 (H_3*C*C=N). IR (drifts): 3071, 2961, 2925, 2869, 1640, 1578, 1571, 1429. MS (EI, *m/z*): 357 $[M^+$, 65], 342 $[M^+ - Me$, 100]. HRMS for $C_{24}H_{27}N_3$ Calc.: 357.2205. Found: 357.2219.

5.2.5. 6,6′-Bis[(2,4,6-trimethylphenylimino)methyl)-2,2′-bipyridine (**6**)

To a solution of 2,4,6-trimethylaniline (0.21 g, 1.5 mmol) and 6,6′-diformyl-2,2′-bipyridine (0.13 g, 0.7 mmol) in 10 ml EtOH was added a drop of AcOH. The mixture was refluxed for 3 h. After cooling down to r.t. the solvent was removed in vaccuo and the yellow solid was washed twice with C_6H_{14}. Compound **6** was isolated as yellow powder in 50% yield (0.15 g).

^{1}H NMR ($CDCl_3$): δ 8.59 (dd, 2H, $J = 1.0$, 7.8 Hz, $H_{5,5'}$), 8.43 (s, 2H, *H*C=N), 8.31 (dd, 2H, $J = 1$, 7.8 Hz, $H_{3,3'}$), 7.94 (t, 2H, $J = 7.8$ Hz, $H_{4,4'}$), 6.92 (s, 4H, Ar*H*), 2.30 (s, 6H, CH_3), 2.17 (s, 12H, CH_3). ^{13}C NMR ($CDCl_3$): δ 163.8 (*C*=N), 155.5, 154.2, 147.9, 137.5, 133.4, 128.8, 126.8, 122.6, 122.6, 121.1, 20.7 (*C*H_3), 18.3 (*C*H_3). MS (EI, *m/z*): 446 $[M^+$, 100]. Elemental analysis for $C_{30}H_{30}N_4$ (446.04) found (required): C, 80.80 (80.68); H, 6.66 (6.77); N, 12.67% (12.55). IR (KBr, cm^{-1}): 1644 (s, ν(C=N)).

5.2.6. 2,9-Bis((2,6-diisopropylphenylimino)methyl)-phenanthroline (**7**)

To a solution of 2,6-diisopropylaniline (0.90 g, 5.1 mmol) and 2,9-diformyl phenanthroline (0.60 g, 2.5 mmol) in 30 ml EtOH was added a drop of formic acid. The mixture was refluxed for 2 h. The initially white suspension turned into a yellow solution. The product precipitates upon cooling to r.t. Compound **7** was isolated as yellow crystals in 72% yield (1.0 g).

^{1}H NMR ($CDCl_3$): δ 8.75 (d, 4H, $H_{3,4,7,8}$), 8.46 (d, 2H, $H_{5,6}$), 7.98 (s, 2H, *H*C=N), 7.1–7.2 (m, 6H, Ar*H*), 3.10 (sept, $J = 6.8$ Hz, 4H, C*H*$(CH_3)_2$), 1.19 (d, $J = 6.8$ Hz, 24H, CH(CH_3)$_2$). ^{13}C NMR ($CDCl_3$): δ 163.1 (*C*=N), 154.9, 148.1, 145.7, 137.2, 137.0, 130.2, 127.8, 124.6, 123.0, 120.6 (Ar*C* and phen*C*), 27.9 (*C*H$(CH_3)_2$), 23.3 (CH(*C*H_3)$_2$). IR (neat, cm^{-1}): 1638 (s, ν(C=N)). MS (EI, *m/z*): 554 $[M^+$, 100], 539 $[M^+ - Me$, 20]. Elemental analysis for $C_{38}H_{42}N_4 \cdot 0.5H_2O$ (563.79) found (required): C, 80.87 (80.96); H, 7.73 (7.69); N, 9.88% (9.94).

5.3. Synthesis of complexes

5.3.1. 2-((2,6-Diisopropylphenylimino)methyl)pyridine nickel dibromide [(**1a**)$NiBr_2$]

Dichloromethane (approximately 30 ml) was added to a mixture of **1a** (0.45 g, 1.70 mmol) and (dme)$NiBr_2$ (0.50 g, 1.60 mmol) in a Schlenk vessel. The mixture was stirred for 18 h during which time an orange precipitate was formed. This precipitate was isolated by filtration, washed with 3 × approximately 10 ml Et_2O and dried in vacuo (0.50 g, 64%). Crystals suitable for X-ray diffraction were grown from a saturated MeCN solution. Elemental analysis for $C_{18}H_{19}Br_2N_2Ni$ (481.87) found (required): C, 44.43 (44.55); H, 4.34 (4.78); N, 5.79% (5.77). IR data (Nujol, KBr, cm^{-1}): 1594(s), 1572(m), 1491(m), 1461(s), 1378(m), 1304(m), 1026(m), 813(m), 772(s), 722(w). FABMS (*m/z*, for ^{79}Br): 880 $[2M - Br]^+$, 480 $[M]^+$. *Crystal data for* [(**1a**)$NiBr_2$(MeCN)]·MeCN: $C_{20}H_{25}Br_2N_3Ni \cdot MeCN$, $M = 567.0$, triclinic, $P\bar{1}$ (no. 2), $a = 7.243(2)$, $b = 10.750(1)$, $c = 16.914(2)$ Å, $\alpha = 88.43(1)$, $\beta = 84.05(1)$, $\gamma = 72.12(1)^\circ$, $V = 1246.4(2)$ Å^3, $Z = 2$, $D_{calc} = 1.511$ g cm^{-3}, μ(Cu Kα) = 4.98 mm^{-1}, $T = 293$ K, orange needles; 3698 independent measured reflections, F^2 refinement, $R_1 = 0.041$, $wR_2 = 0.104$, 3172 independent observed absorption corrected reflections [$|F_o| > 4\sigma(|F_o|)$, $2\theta \leq 120^\circ$], 263 parameters.

5.3.2. ((2,6-Diisopropylphenylimino)methyl)pyrazine nickel dibromide [(**2**)$NiBr_2$]

An analogous procedure to that described for [(**1a**)$NiBr_2$] was followed, using **2** (0.43 g, 1.6 mmol) and (dme)$NiBr_2$ (0.50 g, 1.6 mmol). Compound [(**2**)$NiBr_2$] was isolated as an orange powder in 75% yield (0.6 g).

IR data (Nujol, KBr, cm^{-1}): 1622, 1463, 1186, 1043, 807. FABMS (*m/z*, for ^{79}Br): 822 $[2M - Br]^+$, 401 $[M - Br]^+$. Elemental analysis for $C_{17}H_{18}Br_2N_3Ni$ (482.86) found (required): C, 41.84 (42.02); H, 4.31 (4.36); N, 8.35% (8.64).

*5.3.3. 2-((2,6-Diisopropylphenylimino)methyl)quinoline nickel dibromide [(**3**)$NiBr_2$]*

An analogous procedure to that described for [(**1a**)$NiBr_2$] was followed, using **3** (0.64 g, 2.02 mmol) and (dme)$NiBr_2$ (0.62 g, 2.02 mmol). Compound [(**3**)$NiBr_2$] was isolated as an orange powder in 66% yield (0.71 g). X-ray quality crystals were grown from a concd. CH_2Cl_2 solution.

IR data (Nujol, KBr, cm^{-1}): FABMS (*m*/*z*, for ^{79}Br): 455 $[M-Br,\ 100]^+$, 374 $[M-2Br,\ 50]^+$. Elemental analysis for $C_{22}H_{24}Br_2N_2Ni$ (534.96) found (required): C, 49.51 (49.40); H, 4.76 (4.52); N, 4.98% (5.24). *Crystal data for* [(**3**)$NiBr_2$]: $C_{22}H_{24}Br_2N_2Ni$, $M = 535.0$, monoclinic, $P2_1/n$ (no. 14), $a = 10.064(1)$, $b = 18.239(4)$, $c = 12.244(1)$ Å, $\beta = 99.90(1)^\circ$, $V = 2214.1(6)$ $Å^3$, $Z = 4$, $D_{calc} = 1.605$ g cm^{-3}, μ(Mo Kα) = 4.49 mm^{-1}, $T = 293$ K, deep orange/red prisms; 3857 independent measured reflections, F^2 refinement, $R_1 = 0.055$, $wR_2 = 0.119$, 2391 independent observed absorption corrected reflections [$|F_o| > 4\sigma(|F_o|)$, $2\theta \leq 50^\circ$], 244 parameters.

*5.3.4. 8-((2,6-Diisopropylphenylimino)methyl)quinoline nickel dibromide [(**4**)$NiBr_2$]*

An analogous procedure to that described for [(**1a**)$NiBr_2$] was followed, using **4** (0.32 g, 1.0 mmol) and (dme)$NiBr_2$ (0.31 g, 1.0 mmol). Compound [(**4**)$NiBr_2$] was isolated as an orange powder in 80% yield (0.4 g).

IR data (Nujol, KBr, cm^{-1}): 1628(vs), 1603(vs), 1591(vs), 1580(s), 1516(m), 1464(vs), 1378(s), 1322(w), 1303(w), 1263(m), 1211(w), 1168(s), 1141(w), 1106(m), 1060(w), 1042(w), 1019(w), 1002(w), 986(w), 963(w), 928(m), 887(m), 861(w), 838(m), 804(vs), 781(s), 773(s), 735(m), 724(w). FABMS (*m*/*z*, for ^{79}Br): 986 $[2M-Br]^+$, 532 $[M]^+$. Elemental analysis for $C_{44}H_{48}Br_4N_4Ni_2 \cdot H_2O$ (1087.93) found (required): C, 48.58 (48.58); H, 4.49 (4.63); N, 5.06% (5.15).

*5.3.5. 2-((2,6-Diisopropylphenylimino)methyl)pyridine nickel dimethyl [(**1a**)$NiMe_2$]*

To a stirred suspension of [(**1a**)$NiBr_2$] (0.36 g, 0.74 mmol) in 20 ml Et_2O at -30 °C, MeMgBr (0.5 ml of 3.0 M solution in Et_2O, 1.5 mmol) was added dropwise. This was stirred for 2 h during which time the solution was allowed to warm to 0 °C. After this time the solution became a deep blue/green color. 1,4-Dioxane (approximately 5 ml) was added and a fine precipitate of 1,4-dioxane·$MgBr_2$ formed. The solution was filtered and the solvent removed under reduced pressure. The resultant solid was washed with 3 × approximately 10 ml C_5H_{12}, redissolved in 5 ml Et_2O and cooled to -30 °C to yield highly air and moisture sensitive small dark green blocks. Compound [(**1a**)$NiMe_2$] was also found to be temperature sensitive and decomposes slowly in solution or solid state at ambient temperature.

Yield: 0.18 g (70%). ^1H NMR (250 MHz, CD_2Cl_2, 298 K): δ 8.86 (m, 1H, py–*H*), 8.40 (s, 1H, N=C*H*), 8.06 (m, 1H, py–*H*), 7.78–7.64 (overlapping m, 1H each, py–*H*), 7.36–7.20 (m, 3H, Ar–*H*), 3.22 (sept, 2H, $J = 6.7$ Hz, C*H*$(CH_3)_2$), 1.26 (d, 6H, $J = 6.7$ Hz, CH(CH_3Me′), 1.12 (d, 6H, $J = 6.7$ Hz, CHMe(CH_3)′), 0.40, -0.14 (s, 3H each, Ni–CH_3). ^{13}C NMR (63 MHz, CD_2Cl_2, 298 K): δ 164.3 (imine–*C*), 149.9, 148.8, 139.7, 139.3, 129.4, 127.4, 123.9, 123.4 (py– and Ar–*C*), 28.2 (*C*HMe_2), 22.9, 22.7 (CH(*C*H_3)$_2$), -0.1, -5.9 (Ni–*C*). IR (Nujol, KBr, cm^{-1}): 1610(m), 1580(m), 1558(w), 1539(w), 1462(m), 1376(m), 1354(s), 1331(m), 1300(m), 1274(w), 1216(w), 1183(m), 1156(s), 1101(m), 1061(m), 1039(m), 1018(s), 981(w), 966(w), 944(w), 934(w), 800(s), 772(s), 721(m). MS (EI, *m*/*z*): 356 $[M]^+$. Due to the high air/moisture sensitivity of this compound, satisfactory elemental analysis could not be obtained.

*5.3.6. ((2,6-Diisopropylphenylimino)methyl)pyrazine nickel dimethyl [(**2**)$NiMe_2$]*

An analogous method to that described for compound [(**1a**)$NiMe_2$] was followed using compound [(**2**)$NiBr_2$] (0.36 g, 0.74 mmol) and MeMgBr (0.5 ml of 3.0 M solution in Et_2O, 1.5 mmol). Compound [(**2**)$NiMe_2$] was isolated as a highly air, moisture and temperature sensitive blue/green solid in 60% yield (0.15 g).

IR (Nujol, KBr, cm^{-1}): 1620(w), 1600(m), 1596(m), 1571(w), 1506(w), 1461(s), 1410(m), 1378(s), 1365(s), 1327(m), 1302(w), 1177(w), 1147(w), 1109(w), 1033(m), 982(w), 957(w), 944(w), 933(w), 911(w), 849(w), 831(w), 806(m), 777(w), 745(w), 711(w). MS (FAB^+, *m*/*z*): 356 $[M]^+$. ^1H NMR (250 MHz, CD_2Cl_2, 298 K): δ 9.20 (m, 1H, pyz–*H*), 9.12 (m, 1H, pyz–*H*), 8.88 (m, 1H, pyz–*H*), 8.46 (s, 1H, N=C*H*), 7.36–7.18 (m, 3H, Ar–H), 3.10 (sept, 2H, $^2J = 6.7$ Hz, CH$(CH_3)_2$), 1.22 (d, 6H, $^2J = 6.7$ Hz, CH(CH_3)Me′), 1.08 (d, 12H, $^2J = 6.7$ Hz, CHMe(CH_3)′), 0.60, -0.24 (s, 3H each, Ni–CH_3). ^{13}C NMR (63 MHz, CD_2Cl_2, 298 K): δ 164.3 (imine–C), 150.1, 146.4, 144.5, 139.8, 138.7, 128.1, 123.6 (pyz– and Ar–C), 28.3 (CHMe_2), 24.9, 22.6 (CH$(CH_3)_2$), 0.9, -7.6 (Ni–C). Due to the high air/moisture sensitivity of this compound, satisfactory elemental analysis could not be obtained.

*5.3.7. [2-((2,6-Diisopropylphenylimino)methyl)pyridine nickel methyl diethyletherate]{tetrakis[3,5-bis(trifluoromethyl)phenyl]borate} [(**1a**)$NiMe]^+$*

Diethyl ether (2 ml) was added to [(**1a**)$NiMe_2$] (17.8 mg, 0.05 mmol) and $[H(OEt_2)_2]BArF$ (BArF = [B(3,5-$(CF_3)_2C_6H_3)_4$]–) (50.6 mg, 0.05 mmol) at 0 °C in a Schlenk vessel. A dark red solution formed almost immediately which was stirred for 5 min. After this time solvent was removed under reduced pressure to yield the cationic complex as a dark red solid. All of this product was taken up into approximately 1 ml CD_2Cl_2,

transferred to an NMR tube and the NMR spectrum recorded immediately (>95% by ^{1}H NMR spectroscopy).

^{1}H NMR (250 MHz, CD_2Cl_2, 298 K): δ 8.86 (m, 1H, py–*H*), 8.40 (s, 1H, N=C*H*), 8.06 (m, 1H, py–*H*), 7.78–7.64 (m, 10H, py–*H* and BArF *ortho*-*H*), 7.56 (4H, BArF *para*-*H*), 7.36–7.20 (m, 3H, Ar–*H*), 3.42–3.20 (m, 6H, O(CH_2CH$_3$)$_2$ and C*H*(CH$_3$)$_2$), 1.29–1.18 (m, 12H, O(CH$_2$CH_3)$_2$ and CH(CH_3)Me′), 1.12 (d, 6H, CHMe(CH_3)′), −0.30 (s, 3H, Ni–CH_3). ^{13}C NMR (63 MHz, CD_2Cl_2, 298 K): δ (some signals obscured by BArF resonances) 169.8 (imine–*C*), 162.2 (q, J_{CB} = 37.5 Hz, BArF *ipso*-C), 149.9, 142.2, 141.0, 140.3, 131.5, 118.5 (py– and Ar–*C*), 135.3 (BArF *ortho*-C), 129.3 (q, J_{CF} = 31.3 Hz, BArF *meta*-C), 125.0 (q, J_{CF} = 272.4 Hz, BArF CF_3), 66.5 O(*C*H$_2$CH$_3$)$_2$), 28.5 (*C*H(Me)$_2$), 24.6, 22.6 (CH(*C*H$_3$)$_2$), 15.2 (O(CH$_2$*C*H$_3$)$_2$), 3.4 (Ni–*C*).

5.3.8. [((2,6-Diisopropylphenylimino)methyl)pyrazine nickel methyl diethyletherate]{tetrakis[3,5-bis(trifluoromethyl)phenyl]borate} [(**2**)NiMe]$^+$

An analogous method to that described for compound [(**1a**)NiMe]$^+$ was followed using compound [(**2**)NiMe$_2$] (17.8 mg, 0.05 mmol) and [H(OEt$_2$)$_2$]BArF (50.6 mg, 0.05 mmol) (yield >90% by ^{1}H NMR spectroscopy).

^{1}H NMR (250 MHz, CD_2Cl_2, 298 K): δ 9.28 (m, 1H, pyz–*H*), 9.16 (m, 1H, pyz–*H*), 8.94 (m, 1H, pyz–*H*), 8.48 (s, 1H, N=C*H*), 7.71 (s, 8H, BArF *ortho*-*H*), 7.56 (s, 4H, BArF *para*-*H*), 7.38–7.18 (m, 3H, Ar–*H*), 3.44–3.20 (m, 6H, O(CH_2CH$_3$)$_2$ and C*H*(CH$_3$)$_2$), 1.30–1.16 (m, 12H, O(CH$_2$CH_3)$_2$ and CH(CH_3)Me′), 1.10 (d, 6H, CHMe(CH_3)′), 0.02 (s, 3H, Ni–CH_3). ^{13}C NMR (63 MHz, CD_2Cl_2, 298 K): δ (some signals obscured by BArF resonances) 165.8 (imine–*C*), 162.2 (q, J_{CB} = 37.5 Hz, BArF *ipso*-C), 150.6, 146.8, 146.0, 139.8 (pyz– and Ar–*C*), 135.3 (BArF *ortho*-C) 129.3 (q, J_{CF} = 31.3 Hz, BArF *meta*-C), 125.0 (q, J_{CF} = 272.4 Hz, BArF CF_3), 66.3 (O(*C*H$_2$CH$_3$)$_2$), 28.2 (*C*HMe$_2$), 24.8, 22.6 (CH(*C*H$_3$)$_2$), 15.2 (O(CH$_2$*C*H$_3$)$_2$), 2.4 (Ni–*C*).

5.3.9. 6-[1-(2,6-Diisopropylphenylimino)ethyl]-2,2′-bipyridine iron dichloride [(**5**)FeCl$_2$]

To a solution of $FeCl_2$ (0.12 g, 0.98 mmol) in n-BuOH at 80 °C was added 1 equiv. of the imine ligand (0.35 g, 0.98 mmol). The mixture was stirred at 80 °C for 15 min and allowed to cool to r.t. The solvent was removed in vacuo and the residue washed with Et_2O (2 × 15 ml) to provide a blue solid in 76% yield (0.36 g).

MS (FAB, *m*/*z*): 484 [M^+, 15], 348 [M^+ −Cl, 100]. Elemental analysis for $C_{24}H_{27}Cl_2FeN_3$ (484.25) found (required): C, 59.40 (59.53); H, 5.52 (5.62); N, 8.49% (8.68). μ_{eff} (Evans' balance) = 5.5 BM.

5.4. 6,6′-Bis[(2,4,6-trimethylphenylimino)methyl]-2,2′-bipyridine iron dichloride [(**6**)FeCl$_2$]

To a solution of $FeCl_2$ (25 mg, 0.20 mmol) in 10 ml thf was added 1 equiv. of the imine ligand **6** (92 mg, 0.20 mmol). The mixture was stirred at r.t. overnight. The solvent was removed in vacuo and the residue washed with C_5H_{12} (2 × 15 ml) to provide a green/brown solid in 68% yield (0.80 g).

MS (FAB, *m*/*z*): 572 [M^+, 23], 537 [M^+ −Cl, 100]. Elemental analysis for $C_{30}H_{30}Cl_2FeN_4$ (573.35) found (required): C, 62.46 (62.85); H, 5.50 (5.27); N, 8.95% (9.77). IR (KBr, cm^{-1}): 1634 (broad). μ_{eff} (Evans' NMR method) = 5.0 BM. *Crystal data for* [(**6**)FeCl$_2$]: $C_{30}H_{30}Cl_2FeN_4 \cdot 2CH_2Cl_2$, M = 743.2, tetragonal, $I4_1/a$ (no. 88), a = 23.420(4), c = 26.735(3) Å, V = 14664(3) Å^3, Z = 16, D_{calc} = 1.346 g cm^{-3}, μ(Mo Kα) = 0.88 mm^{-1}, T = 173 K, very dark olive green prisms; 5377 independent measured reflections, F^2 refinement, R_1 = 0.081, wR_2 = 0.174, 2537 independent observed reflections [$|F_o| > 4\sigma(|F_o|)$, $2\theta \leq 47°$], 419 parameters.

5.5. 1,9-Bis[(2,6-diisopropylphenylimino)methyl]-phenanthroline iron dichloride [(**7**)FeCl$_2$]

To a solution of $FeCl_2$ (48 mg, 0.38 mmol) in thf was added 1 equiv. of the imine ligand **7** (0.21 g, 0.38 mmol). The mixture was stirred at r.t. overnight. The solvent was removed in vacuo and the residue washed with Et_2O (2 × 15 ml) to provide a green/brown solid in 73% yield (0.19 g).

MS (FAB, *m*/*z*): 680 [M^+, 40], 645 [M^+ −Cl, 100]. IR (NaCl, cm^{-1}): 1635 (s, ν(C=N) uncoordinated) and 1615 (s, ν(C=N) coordinated). Elemental analysis for $C_{38}H_{42}Cl_2FeN_4$ (681.54) found (required): C, 67.12 (66.97); H, 6.34 (6.21); N, 8.18% (8.22). μ_{eff} (Evans' NMR method) = 5.1 BM.

6. Supplementary material

Crystallographic data for the structural analysis have been deposited with the Cambridge Crystallographic Data Centre, CCDC Nos. 195300–195302 for compounds (**1a**)NiBr$_2$, (**3**)NiBr$_2$ and (**6**)FeCl$_2$. Copies of this information may be obtained free of charge from The Director, CCDC, 12 Union Road, Cambridge, CB2 1EZ, UK (fax: +44-1223-336-033; e-mail: deposit@ccdc.cam.ac.uk or www: http://www.ccdc.cam.ac.uk).

Acknowledgements

Dr. Jane Boyle is thanked for NMR polymer analysis and Dr. Gary Audley is thanked for GPC analysis. We

are grateful for financial support from EPSRC and BP Chemicals Ltd.

References

[1] G.J.P. Britovsek, V.C. Gibson, D.F. Wass, Angew. Chem., Int. Ed. Engl. 38 (1999) 428.
[2] S.D. Ittel, L.K. Johnson, M. Brookhart, Chem. Rev. 100 (2000) 1169.
[3] S. Mecking, Angew. Chem., Int. Ed. Engl. 40 (2001) 534.
[4] L.K. Johnson, C.M. Killian, M. Brookhart, J. Am. Chem. Soc. 117 (1995) 6414.
[5] D.P. Gates, S.A. Svejda, E. Oñate, C.M. Killian, L.K. Johnson, P.S. White, M. Brookhart, Macromolecules 33 (2000) 2320.
[6] L.K. Johnson, C.M. Killian, S.D. Arthur, J. Feldman, E.F. McCord, S.J. McLain, K.A. Kreutzer, M.A. Bennett, E.B. Coughlin, S.D. Ittel, A. Parthasarathy, D.J. Tempel, M.S. Brookhart, DuPont, WO 96/23010, 1996.
[7] B.L. Small, M. Brookhart, A.M.A. Bennett, J. Am. Chem. Soc. 120 (1998) 4049.
[8] B.L. Small, M. Brookhart, Polym. Prep. (Am. Chem. Soc., Div. Polym. Chem.) 39 (1998) 213.
[9] A.M.A. Bennett, DuPont, WO 98/27124, 1998.
[10] G.J.P. Britovsek, V.C. Gibson, B.S. Kimberley, P.J. Maddox, S.J. McTavish, G.A. Solan, A.J.P. White, D.J. Williams, Chem. Commun. (1998) 849.
[11] G.J.P. Britovsek, M. Bruce, V.C. Gibson, B.S. Kimberley, P.J. Maddox, S. Mastroianni, S.J. McTavish, C. Redshaw, G.A. Solan, S. Strömberg, A.J.P. White, D.J. Williams, J. Am. Chem. Soc. 121 (1999) 8728.
[12] G.J.P. Britovsek, B.A. Dorer, V.C. Gibson, B.S. Kimberley, G.A. Solan, BP Chemicals Ltd., WO 99/12981, 1999.
[13] C.M. Killian, L.K. Johnson, M. Brookhart, Organometallics 16 (1997) 2005.
[14] S.A. Svejda, M. Brookhart, Organometallics 18 (1999) 65.
[15] S. Strömberg, M. Oksman, L. Zhang, K. Zetterberg, Acta Chem. Scand. 49 (1995) 689.
[16] B.L. Small, M. Brookhart, J. Am. Chem. Soc. 120 (1998) 7143.
[17] M.S. Brookhart, B.L. Small, DuPont/UNC, WO 99/02472, 1999.
[18] G.J.P. Britovsek, S. Mastroianni, G.A. Solan, S.P.D. Baugh, C. Redshaw, V.C. Gibson, A.J.P. White, D.J. Williams, M.R.J. Elsegood, Chem. Eur. J. 6 (2000) 2221.
[19] C.-Y. Wu, H.E. Swift, J. Catal. 24 (1972) 510.
[20] W. Keim, R. Appel, A. Storeck, C. Krüger, R. Goddard, Angew. Chem., Int. Ed. Engl. 20 (1981) 116.
[21] W. Keim, R. Appel, S. Gruppe, F. Knoch, Angew. Chem., Int. Ed. Engl. 26 (1987) 1012.
[22] C. Wang, S. Friedrich, T.R. Younkin, R.T. Li, R.H. Grubbs, D.A. Bansleben, M.W. Day, Organometallics 17 (1998) 3149.
[23] V.C. Gibson, A. Tomov, A.J.P. White, D.J. Williams, Chem. Commun. (2001) 719.
[24] N.A. Cooley, S.M. Green, D.F. Wass, K. Heslop, A.G. Orpen, P.G. Pringle, Organometallics 20 (2001) 4769.
[25] G.J.P. Britovsek, V.C. Gibson, S. Mastroianni, D.C.H. Oakes, C. Redshaw, G.A. Solan, A.J.P. White, D.J. Williams, Eur. J. Inorg. Chem. (2001) 431.
[26] G.J.P. Britovsek, V.C. Gibson, B.S. Kimberley, S. Mastroianni, C. Redshaw, G.A. Solan, A.J.P. White, D.J. Williams, J. Chem. Soc., Dalton Trans. (2001) 1639.
[27] G.J.P. Britovsek, V.C. Gibson, S.K. Spitzmesser, K.P. Tellmann, A.J.P. White, D.J. Williams, J. Chem. Soc., Dalton Trans. (2002) 1159.
[28] P.-L. Bres, V.C. Gibson, C.D.F. Mabille, W. Reed, D.F. Wass, R.H. Weatherhead, BP Amoco, WO 98/49208, 1998.
[29] R.E. Rülke, J.G.P. Delis, A.M. Groot, C.J. Elsevier, P.W.N.M. van Leeuwen, K. Vrieze, K. Goubitz, H. Schenk, J. Organomet. Chem. 508 (1996) 109.
[30] H. Rutner, P.E. Spoerri, J. Org. Chem. 28 (1963) 1898.
[31] F. Seyhan, J. Org. Chem. 22 (1957) 217.
[32] E.C. Constable, F. Heirtzler, M. Neuburger, M. Zehnder, J. Am. Chem. Soc. 119 (1997) 5606.
[33] S.P.D. Baugh, V.C. Gibson, BP Chemicals Ltd., WO 00/58320, 2000.
[34] G.R. Newkome, H.-W. Lee, J. Am. Chem. Soc. 105 (1983) 5956.
[35] C.J. Chandler, L.W. Deady, J.A. Reiss, J. Heterocycl. Chem. 18 (1981) 599.
[36] T. Laine, M. Leskelä, Borealis, WO 00/18776, 2000.
[37] T.V. Laine, U. Piironen, K. Lappalainen, M. Klinga, E. Aitola, M. Leskelä, J. Organomet. Chem. 606 (2000) 112.
[38] S. Plentz Meneghetti, P.J. Lutz, J. Kress, Organometallics 18 (1999) 2734.
[39] D. Onggo, D.C. Craig, D. Rae, H.A. Goodwin, Aust. J. Chem. 44 (1991) 331.
[40] H.A. Goodwin, D.W. Mather, Aust. J. Chem. 27 (1974) 2121.
[41] A. Angeloff, J.-C. Daran, J. Bernadou, B. Meunier, Eur. J. Inorg. Chem. (2000) 1985.
[42] S. Ameerunisha, J. Schneider, T. Meyer, P.S. Zacharias, E. Bill, G. Henkel, Chem. Commun. (2000) 2155.
[43] R. Ziessel, A. Harriman, J. Suffert, M.-T. Youinou, A. De Cain, J. Fischer, Angew. Chem., Int. Ed. Engl. 36 (1997) 2509.
[44] K.R. Kumar, S. Sivaram, Macromol. Chem. Phys. 201 (2000) 1513.
[45] A. Köppl, H.G. Alt, J. Mol. Catal. 154 (2000) 45.
[46] T.-J.J. Kinnunen, M. Haukka, T.T. Pakkanen, T.A. Pakkanen, J. Organomet. Chem. 613 (2000) 257.
[47] J. Feldman, S.J. McLain, A. Parthasarathy, W.J. Marshall, J.C. Calabrese, S.D. Arthur, Organometallics 16 (1997) 1514.
[48] L.K. Johnson, M.A. Bennett, S.D. Ittel, L. Wang, A. Parthasarathy, E. Hauptman, R.D. Simpson, J. Feldman, E.B. Coughlin, DuPont, WO 98/30609, 1998.
[49] M. Sawamoto, Prog. Polym. Sci. 16 (1991) 111.
[50] J.E. Puskas, G. Kaszas, Rubber Chem. Technol. 69 (1996) 462.
[51] S.Y. Desjardins, K.J. Cavell, J.L. Hoare, B.W. Skelton, A.N. Sobolev, A.H. White, W. Keim, J. Organomet. Chem. 544 (1997) 163.
[52] L. Deng, T.K. Woo, L. Cavallo, P.M. Margl, T. Ziegler, J. Am. Chem. Soc. 119 (1997) 6177.
[53] G.M. Lenges, DuPont, WO 00/68280, 2000.
[54] L. Deng, P.M. Margl, T. Ziegler, J. Am. Chem. Soc. 119 (1997) 1094.
[55] T.V. Laine, M. Klinga, M. Leskelä, Eur. J. Inorg. Chem. (1999) 959.
[56] A. Köppl, H.G. Alt, Phillips Petroleum Company, WO 99/49970, 1999.
[57] M. Brookhart, B. Grant, A.F. Volpe, Organometallics 11 (1992) 3920.
[58] A.R. Katritzky, A.F. Pozharskii (Eds.), Handbook of Heterocyclic Chemistry, 2nd ed., Elsevier, Amsterdam, 2000, p. 177.